Studies of the Reactions of Group 8 Transition-Metal Ions Fe^+, Co^+, and Ni^+ with Linear Alkanes. Determination of Reaction Mechanisms and $MC_nH_{2n}^+$ Ion Structures Using Fourier Transform Mass Spectrometry Collision-Induced Dissociation

D. B. Jacobson and B. S. Freiser*

Contribution from the Department of Chemistry, Purdue Univeristy, West Lafayette, Indiana 47907. *Received December 13, 1982*

Abstract: With use of Fourier transform mass spectrometry, the ion products resulting from the reactions of the group 8 transition-metal ions Fe^+, Co^+, and Ni^+ with a variety of hydrocarbons were studied by both collision-induced dissociation and specific ion–molecule reactions. Evidence is provided for four unique $MC_4H_8^+$ structures. All three metal ions dehydrogenate linear alkanes larger than propane via initial insertion into C–C bonds resulting in the formation of bis(olefin)–metal ion complexes. In addition, Fe^+ also dehydrogenates linear alkanes via initial insertion into C–H bonds, producing an olefin–metal ion complex. β-Hydride transfers are more facile for Co^+ than either Fe^+ or Ni^+. Secondary β-hydride transfers are more facile than primary β-hydride transfers for both Co^+ and Ni^+; however, the reverse is observed for Fe^+. Both Co^+ and Ni^+ are highly selective against insertion into terminal C–C bonds, with Fe^+ showing considerably less selectivity. Formation of $MC_4H_6^+$ ions from linear alkanes larger than butane occurs via initial alkane loss producing a metal ion–butene complex followed by dehydrogenation.

Introduction

Transition-metal ions have proven to be highly reactive in the gas phase. This has been demonstrated by several recent investigations on the reactions of gas-phase transition-metal ions with a variety of organic species using ion cyclotron resonance (ICR)[1,2] spectroscopy and ion beam techniques.[3-8] A variety of fundamental thermodynamic, kinetic, and mechanistic information about gas-phase organometallic chemistry can be obtained in these studies. The reactions with hydrocarbons are fundamentally important since only two types of bonds are available for metal insertion: C–H and C–C bonds.

Several metal–methyl, metal–carbene, and metal–hydride bond energies have recently been determined by Beauchamp et al. using an ion beam instrument.[3-7] These bond energies can be of use in explaining the reactivity of metal ions as well as reaction mechanisms. The determination of reaction mechanisms, however, continues to suffer from the fact that ion structures are usually inferred with little experimental evidence available to support the proposed structures. In many cases several reasonable mechanisms can be postulated to explain the formation of reaction products. Determination of ion structures can usually eliminate all but one or two mechanisms. Methods available to the gas-phase chemist for ion structure determination are increasing and include isotopic labeling, reactivity, photodissociation, and collision-induced dissociation (CID). Of these, collision-induced dissociation (CID) is the most useful and widely employed technique for ion structure determination in the gas phase.[9] Freas and Ridge recently demonstrated the potential of CID in studies of $FeC_4H_{10}^+$ and $CrC_4H_{10}^+$ formed by reactions of $FeCO^+$ and $CrCO^+$ with butane using conventional reverse-geometry mass spectrometric techniques.[10] Recently, we reported the use of CID in a Nicolet prototype Fourier transform mass spectrometer (FTMS) to determine the structures of ion products resulting from the reaction of Ni^+ with several alkanes.[11] Determination of these structures resulted in greater insight into reaction mechanisms.

Scheme I

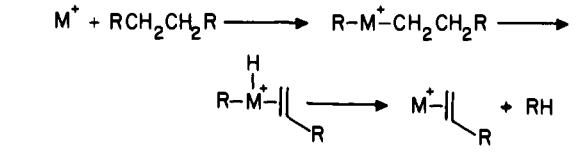

Scheme II

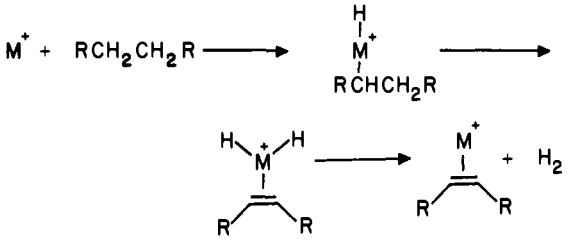

Table I. Neutral Fragment Losses from CID of $MC_4H_8^+$ Complexes (M = Fe, Co, or Ni[a,b])

structure	H_2	C_2H_4	C_4H_8
	×		×
			×
	×	×	×
		×	×

[a] CID fragments observed at 15 eV of kinetic energy. [b] Argon added for total pressure of 1×10^{-5} torr.

(1) (a) Allison, J.; Ridge, D. P. *J. Am. Chem. Soc.* **1979**, *101*, 4998. (b) Allison, J.; Ridge, D. P. *Ibid.* **1976**, *98*, 7445. (c) Allison, J.; Ridge, D. P. *J. Organomet. Chem.* **1975**, *99*, C11. (d) Allison, J.; Freas, R. B.; Ridge, D. P. *J. Am. Chem. Soc.* **1979**, *101*, 1332.

(2) (a) Burnier, R. C.; Byrd, G. D.; Freiser, B. S. *J. Am. Chem. Soc.* **1981**, *103*, 4360. (b) Byrd, G. D.; Burnier, R. C.; Freiser, B. S. *Ibid.* **1982**, *104*, 3565. (c) Byrd, G. D.; Freiser, B. S. *Ibid.* **1982**, *104*, 5944.

(3) Armentrout, P. B.; Beauchamp, J. L. *J. Chem. Phys.* **1981**, *74*, 2819.

(4) Armentrout, P. B.; Beauchamp, J. L. *J. Am. Chem. Soc.* **1981**, *103*, 784.

(5) Armentrout, P. B.; Halle, L. F.; Beauchamp, J. L. *J. Am. Chem. Soc.* **1981**, *103*, 6501.

(6) Armentrout, P. B.; Beauchamp, J. L.; *Chem. Phys.* **1980**, *50*, 37.

(7) Halle, L. F.; Armentrout, P. B.; Beauchamp, J. L. *Organometallics* **1982**, *1*, 963.

(8) (a) Armentrout, P. B.; Halle, L. F.; Beauchamp, J. L. *J. Am. Chem. Soc.* **1981**, *103*, 6624. (b) Armentrout, P. B.; Beauchamp, J. L. *J. Am. Chem. Soc.* **1981**, *103*, 6628.

(9) Cooks, R. G. "Collision Spectroscopy"; Plenum Press: New York, 1978.

(10) Freas, R. D.; Ridge, D. P. *J. Am. Chem. Soc.* **1980**, *102*, 7129.

(11) Jacobson, D. B.; Freiser, B. S. *J. Am. Chem. Soc.* **1983**, *105*, 736.

0002-7863/83/1505-5197$01.50/0

Scheme III

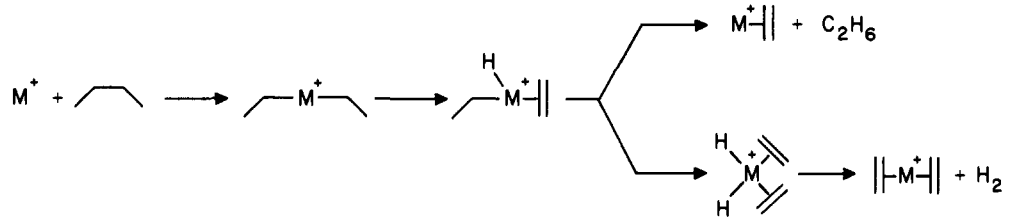

Oxidative addition of a metal ion across a C–C bond is postulated as the initial step in the cleavage of alkanes. This is followed by a β-hydride shift onto the metal and then onto the alkyl portion, resulting in reductive elimination of an alkane and formation of a primary olefin–metal complex (Scheme I). Oxidative addition of a metal ion across a C–H bond is proposed as the initial step in the dehydrogenation of alkanes. This is followed by a β-hydride shift onto the metal with subsequent reductive elimination of hydrogen (a 1,2-elimination process) and formation of an olefin–metal complex (Scheme II), , where the geometry of the olefin is unknown. Recently, Beauchamp et al. reported the surprising result that Ni^+ dehydrogenates *n*-butane exclusively by a highly specific 1,4-elimination mechanism[12] (Scheme III). This mechanism involves initial oxidative addition of Ni^+ not across a C–H bond but rather across an internal C–C bond followed by two successive β-hydride shifts onto the metal with reductive elimination of hydrogen producing a bis(olefin) complex. This mechanism requires that β-hydride shifts be competitive with alkane elimination. In a more extensive study we corroborated Beauchamp's results on butane and showed that the mechanism was general for Ni^+ reacting with alkanes larger than propane.[11] Our conclusions relied heavily on determining the product ion structures by using CID and specific ion–molecule reactions. We demonstrated, for example, that four unique structures of $NiC_4H_8^+$ generated from four different precursors can readily be distinguished. The neutral losses observed in the CID spectrum of each of these $NiC_4H_8^+$ ions are summarized in Table I.

Other metal ions that react with alkanes to produce both cleavage and dehydrogenation products may dehydrogenate linear alkanes by Scheme III or by a combination of Schemes II and III. In this paper, we apply FTMS to the study of the structures of ion products resulting from the reactions of Fe^+ and Co^+ with several alkanes, and these results are then compared to those previously reported for Ni^+.[11] Once again, determination of ion structures provides greater insight into the mechanisms leading to product formation.

Experimental Section

All experiments were performed on a prototype Nicolet FTMS 1000 ICR spectrometer previously described in detail[13,14] and equipped with a 1-in. cubic trapping cell situated between the poles of a Varian 15-in. electromagnet maintained at 0.9 T. The cell has been modified by drilling a $^1/_4$-in. diameter hole in one of the receiver plates, which permits irradiation with various light sources. High purity foils of the appropriate metal were attached to the opposite receiver plate. Metal ions were generated by focusing the beam of a Quanta Ray Nd:YAG laser (frequency doubled to 530 nm) onto the metal foil. Details of the laser ionization technique have been described elsewhere.[2a]

Chemicals were obtained commercially in high purity and used as supplied except for multiple freeze–pump–thaw cycles to remove noncondensable gases. Sample pressures were on the order of 3×10^{-7} torr. Argon was used as the collision gas for the CID experiments at a total sample pressure of approximately 1×10^{-5} torr. A Bayard–Alpert ionization gauge was used to monitor pressure.

Details of the CID experiments have previously been discussed.[11,14] Figure 1 shows the timing sequence used in the CID experiments. A quench pulse that removes all ions present in the cell starts the experiment followed by an ion formation pulse (a 7-ns laser pulse). This is followed by a 500–1000 ms reaction time to allow reaction products to build up. All ions except the ion of interest are then ejected from the cell (DR1 AND DR2) followed by a CID pulse (DR3) that imparts variable kinetic energy to the ion under investigation. There is an additional 25-ms delay after the CID pulse to allow for fragmentation followed by detection to give a complete mass spectrum of the CID products. The CID fragments observed are, for the most part, the result of multiple collisions.[15] The effect of multiple collisions on dissociation pathways is currently under investigation in our laboratory. The major effect of this is that low-energy rearrangements will be favored over more direct processes. These rearrangements are most significant for CID of branched olefin–metal ion complexes.[16] The maximum translational energy acquired by the ion (in excess of thermal energy) is given by eq 1, where e is the electronic charge (1.6×10^{-19} C to give E_{tr} in units of

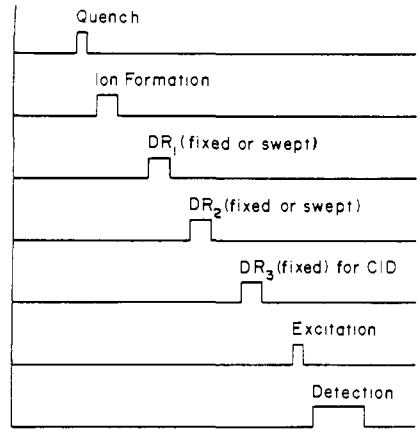

Figure 1. Typical sequence of events for the FTMS CID experiment.

$$E_{tr(max)} = \frac{E_{RF}^2 e t^2}{8m} \quad (1)$$

electron volts), m is the mass of the ion in kilograms, E_{RF} is the amplitude of the irradiation frequency in volts per meter, and t is the time of irradiation in seconds. The time (t) of the irradiation frequency is varied (0.060–0.700 ms) to vary the translational energy of the ions and, hence, the center of mass energy, which is related to the amount of internal energy an ion may obtain upon a collision event at E_{tr}. The spread in ion kinetic energies is dependent on the total average kinetic energy and is approximately 35% at 1 eV, 10% at 10 eV, and 5% at 30 eV.[17] CID efficiencies of 30–50% were observed for all ions studied.

Specific ion–molecule reactions required a timing sequence similar to that of the CID experiments. The metal ion–alkane reaction products are initially formed by using trapping times of 400–600 ms, and the unwanted ions are then ejected, followed by a second trapping time (variable) to allow for ion–molecule reactions to occur.

Results and Discussion

$MC_2H_4^+$ and $MC_3H_6^+$. Fe^+, Co^+, and Ni^+ react with propane to produce $MC_2H_4^+$ (reaction 2) and $MC_3H_6^+$ (reaction 3) as the

$$M^+ + \text{propane} \rightarrow MC_2H_4^+ + CH_4 \quad (2)$$

$$M^+ + \text{propane} \rightarrow MC_3H_6^+ + H_2 \quad (3)$$

(12) Halle, L. F.; Houriet, R.; Kappas, M.; Staley, R. H.; Beauchamp, J. L. *J. Am. Chem. Soc.* **1982**, *104*, 6293.
(13) Cody, R. B.; Freiser, B. S. *Int. J. Mass Spectrom. Ion Phys.* **1982**, *41*, 199.
(14) Cody, R. B.; Burnier, R. C.; Freiser, B. S. *Anal. Chem.* **1982**, *54*, 96.
(15) Burnier, R. C.; Cody, R. B.; Freiser, B. S. *J. Am. Chem. Soc.* **1982**, *104*, 7436.
(16) Jacobson, D. B.; Freiser, B. S. *J. Am. Chem. Soc.* **1983**, *105*, 736.
(17) Huntress, W. T.; Moseman, M. M.; Elleman, D. D. *J. Chem. Phys.* **1971**, *54*, 843.

only primary reaction products. The ions generated in reactions 2 and 3 yield direct cleavage of the organic portions as the only fragmentations observed under CID conditions. Scheme I predicts formation of a metal ion–ethene complex in reaction 2. The product of reaction 3 is a metal ion–propene complex, which Scheme II predicts. An equilibrium between the propene and the hydrido π-allyl complex, I, may exist (reaction 4). The hydrido

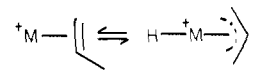

(4)

π-allyl complex was postulated for Rh^+, for example, when the $RhC_3H_6^+$ ion generated in reaction 3 was found to undergo five H/D exchanges in the presence of excess deuterium.[2c] No H/D exchanges, however, were observed for $MC_3H_6^+$ (M = Fe, Co, or Ni) ions generated in reaction 3, suggesting the presence of only the propene structure. The absence of H/D exchanges may be due to the fact that initial oxidative addition of D_2 onto the metal may be endothermic; hence, H/D exchanges would not be observed. Evidence against this is that six H/D exchanges have been observed for $CoC_5H_6^+$.[18] Finally, no H/D exchanges were observed for collisionally activated $MC_3H_6^+$ ions in the presence of Ar (collision gas) with excess deuterium in a controlled-CID-type experiment. These results indicate that the $MC_3H_6^+$ ions generated in reaction 3 retain a rigid propene–metal ion structure.

$MC_4H_8^+$ Ions. Linear alkanes larger than butane can be cleaved by Fe^+, Co^+, and Ni^+ to produce $MC_4H_8^+$ ions (reaction 5, n = 5–8). Dehydrogenation at low kinetic energies along with loss

$$M^+ + n\text{-}C_nH_{2n+2} \rightarrow MC_4H_8^+ + C_{n-4}H_{2n-6} \quad (5)$$

of C_4H_8 at higher kinetic energies are the only fragmentations observed in the CID spectrum of $MC_4H_8^+$ ions generated in reaction 5. As shown in our earlier report on Ni^+ [11] (see Table I), these results provide evidence for a primary butene–metal ion complex, II, which is predicted by Scheme I. A dehydrogenation

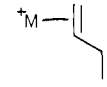

II

mechanism for the activated $MC_4H_8^+$ ions is presented in Scheme IV. Oxidative addition of an allylic C–H bond to the metal forming a hydrido π-allylmetal complex is followed by a β-hydride shift onto the metal with subsequent reductive elimination of hydrogen and formation of a metal ion–butadiene complex. The hydrido π-allylmetal complex has been proposed as an intermediate in solution-phase chemistry[19-21] and for alkene isomerization and hydrogenation on metal surfaces[22] and has also been implicated in the gas-phase chemistry as discussed earlier.

The reaction of Fe^+, Co^+, and Ni^+ with 2,2-dimethylpropane generates an $MC_4H_8^+$ ion as the only primary reaction product (reaction 6). No fragmentations other than loss of C_4H_8 are

$$M^+ + \text{2,2-dimethylpropane} \rightarrow MC_4H_8^+ + CH_4 \quad (6)$$

observed in the CID spectrum of this ion. This is consistent with a 2-methylpropene–metal ion complex, III (see Table I). De-

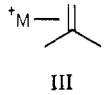

III

hydrogenation of III to form a metal ion–trimethylene methane

Scheme IV

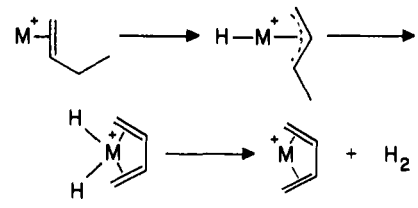

Scheme V

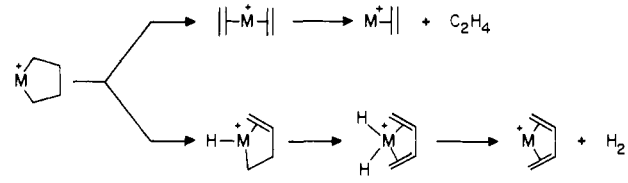

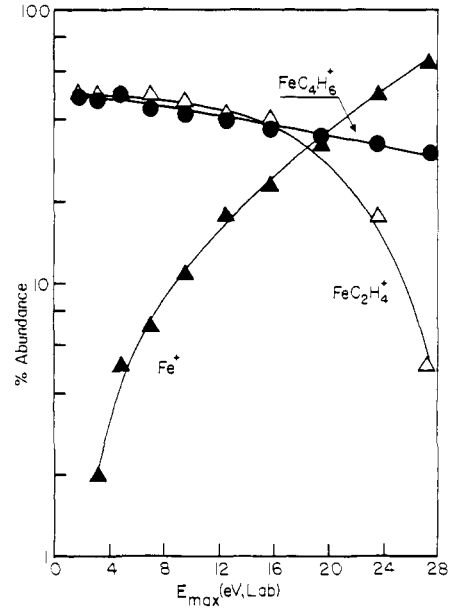

Figure 2. CID product ion intensities vs. kinetic energy for $FeC_4H_8^+$ ions generated in reaction 8.

complex or rearrangement to a metal ion–butadiene complex is not observed. The absence of any cleavages other than loss of C_4H_8 is consistent with the low cross section observed for the reaction of Co^+ with 2-methylpropene as compared to other olefins.[8a]

An ion corresponding to $MC_4H_8^+$ is also formed in the decarbonylation of cyclopentanone[23] by Fe^+, Co^+, and Ni^+ along with three other primary reaction products (reactions 7–10). The

		Fe^+	Co^+	Ni^+	
M^+ + cyclopentanone	$\rightarrow MC_5H_6O^+ + H_2$	11%	5%	0%	(7)
	$\rightarrow MC_4H_8^+ + CO$	30%	8%	39%	(8)
	$\rightarrow MC_4H_6^+ + CO + H_2$	49%	82%	48%	(9)
	$\rightarrow MCO^+ + C_4H_8$	10%	5%	13%	(10)

fragment ion abundances vs. ion kinetic energy resulting from CID of $FeC_4H_8^+$ ions generated in reaction 8 are shown in Figure 2. The intensity of the $CoC_4H_8^+$ ions generated in reaction 8 was too low to allow for structural determination. Reasons for the low abundance of $CoC_4H_8^+$ will be discussed later in the text.

(18) Jacobson, D. B.; Byrd, G. D.; Freiser, B. S. *Inorg. Chem.*, in press.
(19) Tulip, T. H.; Ibers, J. A. *J. Am. Chem. Soc.* **1979**, *101*, 4201.
(20) Ephritikhine, M.; Green, M. L. H.; Mackenzie, R. E. *J. Chem. Soc., Chem. Commun.* **1976**, 619.
(21) Byrne, J. W.; Blasser, H. U.; Osborn, J. A. *J. Am. Chem. Soc.* **1975**, *97*, 3817.
(22) Webb, G. "Catalysis"; Kembal, C., Dowden, D. A., Eds.; The Chemical Society: London, 1977, Vol. 2, pp 151–163.

(23) Studies on the reactions of Fe^+, Co^+, and Ni^+ with ^{18}O-labeled cyclopentanone indicate that decarbonylation is the major process in which a neutral fragment with 28 amu is eliminated by using the unlabeled reactant, accounting for greater than 90% of the product. A minor process results in loss of ethene from the 3,4-sites on the ring (Kalmbach, K. A.; Ridge, D. P., unpublished results). The neutral products of reaction 9 are uncertain. Possibilities are H_2CO or H_2 and CO.

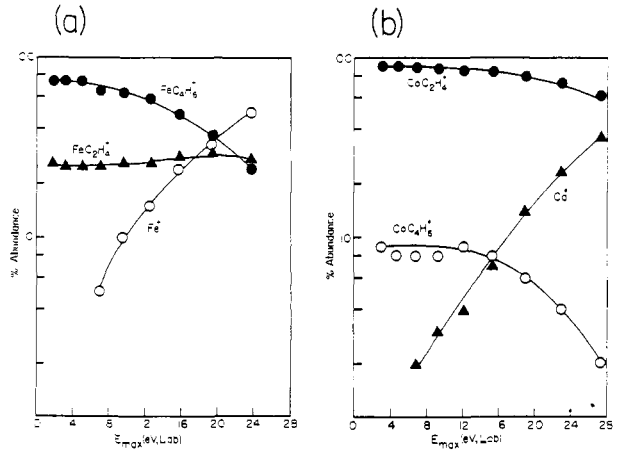

Figure 3. (a) CID product ion intensities vs. kinetic energy for $FeC_4H_8^+$ ions generated in reaction 11. (b) CID product ion intensities vs. kinetic energy for $CoC_4H_8^+$ ions generated in reaction 11.

Dehydrogenation and loss of C_2H_4 are the only fragments observed along with loss of C_4H_8 for both $FeC_4H_8^+$ and $NiC_4H_8^+$ ions. Both ions are unreactive with HCN indicating that the C_4H_8 unit has remained intact.[11,12] A metallacyclopentane, IV, is postulated from

IV

these results. The CID fragmentation pathways are illustrated in Scheme V. Dehydrogenation proceeds via two successive β-hydride shifts onto the metal followed by reductive elimination of hydrogen, producing a metal ion–butadiene complex. Loss of C_2H_4 simply involves rearrangement to a bis(olefin) complex followed by loss of C_2H_4. Loss of C_2H_4 has been observed in the thermal decomposition of metallacyclopentanes in solution.[24-27] Finally, metallacycles have been proposed as intermediates in a number of transition-metal-catalyzed reactions, notably the alkene metathesis reaction.[28-31] The study of metallacycles in the absence of solution effects should prove to be both interesting and informative.

Butane is dehydrogenated by Fe^+, Co^+, and Ni^+ to yield $MC_4H_8^+$ ions (reaction 11). The CID fragmentation abundances

$$M^+ + n\text{-butane} \rightarrow MC_4H_8^+ + H_2 \qquad (11)$$

vs. ion kinetic energy for $FeC_4H_8^+$ and $CoC_4H_8^+$ ions are shown in Figure 3. Furthermore, these $MC_4H_8^+$ ions were reacted with HCN, resulting in sequential displacement of C_2H_4 (reaction 12).

$$MC_4H_8^+ \xrightarrow{HCN} MC_2H_4(HCN)^+ \xrightarrow{HCN} M(HCN)_2^+ \qquad (12)$$

The temporal variation of ion abundances for the reaction of $CoC_4H_8^+$ with HCN is shown in Figure 4. While all of the $NiC_4H_8^+$ ions were observed to undergo sequential C_2H_4 displacement,[11,12] the results in Figure 4 show that about 11% of the $CoC_4H_8^+$ ions remain unreactive. Results for $FeC_4H_8^+$ ions were inconclusive due to competing reactions. Butene–metal ion complexes produced in reactions 5 and 6 were observed to be

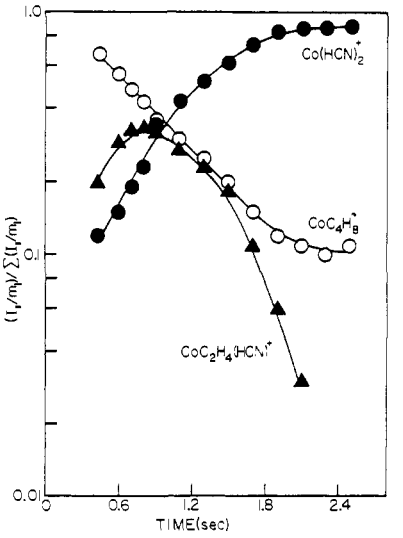

Figure 4. Temporal variation for the reaction of $CoC_4H_8^+$ ions generated in reaction 12 with HCN.

Scheme VI

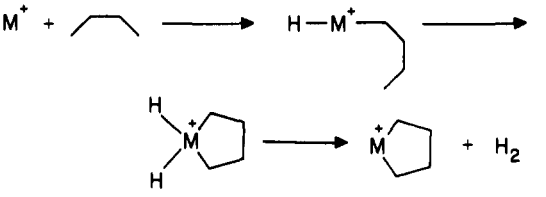

unreactive with HCN. The CID spectra of $NiC_4H_8^+$ produced from butane (reaction 11) consists of 100% loss of C_2H_4, while that of $CoC_4H_8^+$ consists of 90% loss of C_2H_4 and 10% dehydrogenation, and $FeC_4H_8^+$ consists of 30% loss of C_2H_4 and 70% dehydrogenation at low kinetic energies. These results provide evidence for the presence of two different $MC_4H_8^+$ structures generated in reaction 11 for Fe^+ and Co^+ in contrast to Ni^+. Displacement of C_2H_4 by HCN along with loss of C_2H_4 by CID are consistent with a bis(olefin)–metal ion complex, V. Dehydrogenation in the CID spectrum along with the fraction of $CoC_4H_8^+$ that remains unreactive with HCN are consistent with a butene–metal ion complex, II, where the position of the double bond is unknown. These results suggest that Ni^+ dehydrogenates *n*-butane exclusively by Scheme III, Co^+ dehydrogenates *n*-butane 90 ± 5% by Scheme III and 10 ± 5% by Scheme II, and Fe^+ dehydrogenates *n*-butene 30 ± 10% by Scheme III and 70 ± 10% by Scheme II. This assumes that both structures have similar CID cross sections. This assumption seems reasonable since loss of C_2H_4 from V and dehydrogenation of II have similar CID cross sections for Ni^+ and the CID spectra for $CoC_4H_8^+$ ions generated in reaction 11 yield structure distributions similar to those determined by HCN displacement.

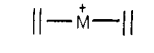

V

Formation of the bis(olefin) complex, V, may proceed via a metallacycle intermediate (Scheme VI). However, there are several compelling reasons to believe that this mechanism is not involved. If a metallacyclopentane is involved in the dehydrogenation of *n*-butane by Ni^+ then it may rearrange to the bis(olefin) complex, V, or dehydrogenate to produce $NiC_4H_6^+$ ions, provided it retained sufficient internal energy. If the metallacycle is stable, then both dehydrogenation to produce $NiC_4H_6^+$ ions along with loss of C_2H_4 to produce $NiC_2H_4^+$ ions would be observed in the CID spectrum. Metallacycles are not involved in the dehydrogenation of *n*-butane by Ni^+ since no $NiC_4H_6^+$ ions are observed as primary reaction products or in the CID spectrum of $NiC_4H_8^+$ ions generated in reaction 11. The arguments for

(24) Grubbs, R. H.; Miyashita, A.; Liu, M.; Burk, P. *J. Am. Chem. Soc.* **1978**, *100*, 2418.
(25) Baterman, P. S. *J. Chem. Soc., Chem. Commun.* **1979**, 70.
(26) Grubbs, R. H.; Miyashita, A.; Liu, M.; Burk, P. L. *J. Am. Chem. Soc.* **1977**, *99*, 3863.
(27) McDermott, J. X.; Wilson, M. E.; Whitesides, G. M. *J. Am. Chem. Soc.* **1976**, *98*, 6529.
(28) Grubbs, R. H. *Prog. Inorg. Chem.* **1978**, *24*, 1.
(29) Grubbs, R. H.; Miyashita, A. "Fundamental Research in Homogeneous Catalysis"; Tsutsui, M., Ed.; Plenum Press: New York, 1979; Vol. 3, p 151.
(30) Herisson, J. L.; Chauvin, Y. *Makromol. Chem.* **1970**, *141*, 161.
(31) Stevens, A. E.; Beauchamp, J. L. *J. Am. Chem. Soc.* **1979**, *101*, 6449.

Scheme VII

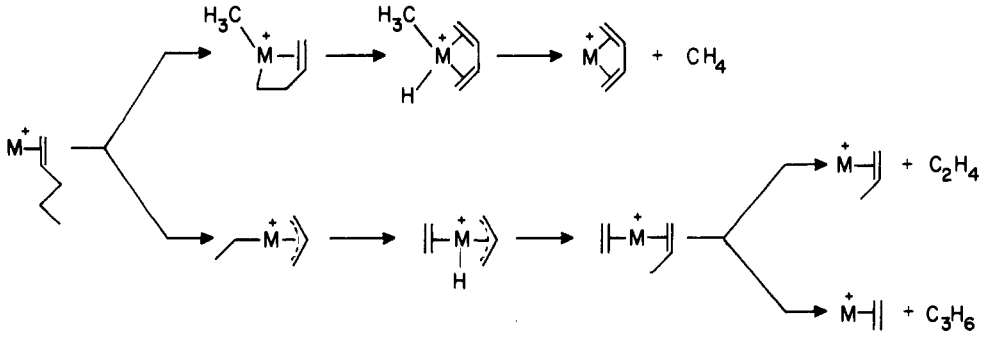

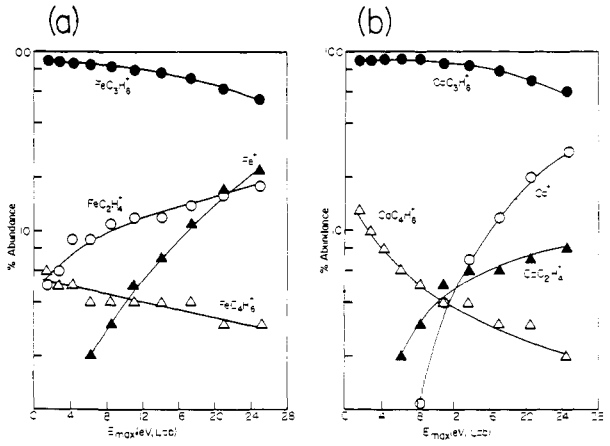

Figure 5. (a) CID product ion intensities vs. kinetic energy for $FeC_5H_{10}^+$ ions generated from *n*-heptane (reaction 14). (b) CID product ion intensities vs. kinetic energy for $CoC_5H_{10}^+$ ions generated from *n*-heptane (reaction 14).

Co^+ and Fe^+ are not as strong; however, dehydrogenation via a metallacycle intermediate (Scheme VI) is considered highly unlikely.

Metallacycles have been synthesized in solution by olefin dimerization reactions.[32-39] Metallacyclopentanes have also been observed to be in equilibrium with their bis(olefin) counterparts[40,41] (reaction 13). If this equilibrium is occurring in the gas phase,

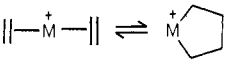

(13)

then the bis(ethene)nickel ions, V, would be expected to show some dehydrogenation in the CID spectrum of V since the nickelacyclopentane structure dehydrogenates to yield $NiC_4H_6^+$ ions under CID conditions. This equilibrium is not observed in the gas phase for Ni^+ since no dehydrogenation of $NiC_4H_8^+$ ions generated in reaction 11 is observed in its CID spectrum. This equilibrium cannot be ruled out for either Co^+ or Fe^+; however, it also seems unlikely.

Table II. Neutral Products Lost in the Primary Reactions of Fe^+, Co^+, and Ni^+ with Alkenes[a]

		neutral fragments lost, %					
alkene	M^+	H_2	CH_4	C_2H_4	C_3H_6	C_4H_8	C_2H_6
1-pentene	Fe	13	19	49	19		
	Co	5	7	67	21		
	Ni		3	74	24		
1-hexene	Fe	11	2	12	61	7	7
	Co	4	2	3	78	4	9
	Ni		2	2	82	5	9

[a] All numbers are ±10% of absolute.

$MC_5H_{10}^+$. $MC_5H_{10}^+$ ions are produced in the reaction of Fe^+, Co^+, and Ni^+ with linear alkanes larger than pentane (reaction 14, n = 6–8). Scheme I predicts the formation of a primary

$$M^+ + n\text{-}C_nH_{2n+2} \rightarrow MC_5H_{10}^+ + C_{n-5}H_{2n-8} \qquad (14)$$

pentene–metal ion complex, VI. The fragmentation abundances

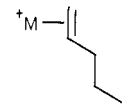

VI

vs. ion kinetic energy for CID of $FeC_5H_{10}^+$ and $CoC_5H_{10}^+$ ions generated by reaction with *n*-heptane are shown in Figure 5. Plots of CID fragmentation abundances vs. ion kinetic energy for $MC_5H_{10}^+$ ions generated from reactions with *n*-hexane and *n*-octane were reproducible to within ±5% absolute at all kinetic energies studied compared to that for *n*-heptane. Losses of C_2H_4, C_3H_6, and CH_4 are observed, and in contrast to the primary butene results, no dehydrogenation is seen for any of the $MC_5H_{10}^+$ ions. Only losses of C_2H_4 and C_3H_6 were seen for $NiC_5H_{10}^+$ ions generated in reaction 14.[11] A mechanism for these losses is outlined in Scheme VII. Oxidative addition of a terminal C–C bond or an allylic C–C bond initially occurs. This is followed by a β-hydride transfer across the metal, resulting in reductive elimination of CH_4, producing a metal ion–butadiene complex in the former and formation of a bis(olefin) complex in the latter. This bis(olefin) complex can then eliminate either C_2H_4 or C_3H_6. Loss of C_2H_4 dominates over loss of C_3H_6 at all kinetic energies, with the greatest dominance at the lowest collision energies. This is consistent with larger olefins being bound more strongly to metal ion centers than smaller olefins,[42] and hence, smaller olefins will be preferentially cleaved from bis(olefin) complexes.

Conversion of 1-pentene to butadiene and methane or propene and ethene requires 13.5 and 22.4 kcal/mol, respectively.[43] In addition, butadiene will be bound more strongly to the metal center than 1-pentene;[4,43] hence, insertion into the terminal C–C bond of VI produces thermally more stable products than insertion into

(32) Noyori, R.; Kumagai, Y.; Tahaya, H. *J. Am. Chem. Soc.* **1974**, *96*, 634.
(33) Kata, T.; Cerefice, S. *J. Am. Chem. Soc.* **1969**, *91*, 6519.
(34) McMeeking, D.; Binger, P. *J. Chem. Soc., Chem. Commun.* **1976**, 376.
(35) Cassar, L.; Eaton, P. E.; Halpern, J. *J. Am. Chem. Soc.* **1970**, *92*, 3515.
(36) Chatt, J.; Haines, R. J.; Leigh, G. J. *J. Chem. Soc., Chem. Commun.* **1972**, 1203.
(37) Fraser, A. R.; Bird, P. H.; Bezman, S. A.; Shapley, J. R.; White, R.; Osborn, J. A. *J. Am. Chem. Soc.* **1973**, *95*, 597.
(38) Porri, L. *Tetrahedron Lett.* **1974**, 879.
(39) McDermott, J. X.; White, J. F.; Whitesides, G. M. *J. Am. Chem. Soc.* **1973**, *95*, 4451.
(40) Grubbs, R. H.; Miyashita, A. *J. Am. Chem. Soc.* **1978**, *100*, 1300.
(41) McLain, S. J.; Wood, C. D.; Schrock, R. R. *J. Am. Chem. Soc.* **1977**, *99*, 3519.
(42) Kappas, M. M.; Staley, R. H. *J. Am. Chem. Soc.* **1982**, *104*, 1813.
(43) Thermochemical information is taken from the following: Stull, D. R.; Westrum, E. F.; Sinke, G. C. "Chemical Thermodynamics of Organic Compounds"; Wiley: New York, 1969.

the allylic C–C bond. The small fraction of terminal C–C bond insertion (Figure 5) indicates that either a high-energy intermediate is involved or the frequency factor for insertion into the allylic C–C bond is much higher than that for the terminal C–C bond. As seen above, linear butene–metal ion complexes readily dehydrogenate producing butadiene–metal ion complexes, probably because rearrangement via Scheme VII is not possible for butene–metal ion complexes. The absence of any dehydrogenation of VI indicates that insertion into C–C bonds is considerably more facile than C–H bond insertion for activated 1-pentene–metal ion complexes.

These CID results can be compared with the primary reaction products observed in the reactions of Fe^+, Co^+, and Ni^+ with 1-pentene (Table II). These results are similar to the CID fragmentations seen in Figure 5. Presumably, the metal ions initially coordinate to the site of unsaturation followed by rearrangements outlined in Scheme VII. Interestingly, dehydrogenation to form $MC_5H_8^+$ ions is observed in the reaction of both Co^+ and Fe^+ with 1-pentene but not in their CID spectra. This may be due to insertion of the metal ion into C–H bonds prior to olefin coordination. Alternatively, the nature of the CID experiment (multiple collisions) may allow the ions to gain internal energy in a stepwise fashion favoring lower energy processes. The CID spectra of $MC_5H_{10}^+$ ions resulting from displacement of smaller olefins by 1-pentene are, within experimental error, identical with those in Figure 5, providing further evidence for the integrity of structure VI from reaction 14.

Fe^+, Co^+, and Ni^+ dehydrogenate pentane to produce $MC_5H_{10}^+$ ions, reaction 15. Insertion into C–C bonds by M^+ should become

$$M^+ + n\text{-pentane} \rightarrow MC_5H_{10}^+ + H_2 \qquad (15)$$

even more competitive with C–H bond insertion in pentane compared to butane since internal C–C bonds become weaker as the size of the alkane chain increases. Hence, Ni^+ should dehydrogenate *n*-pentane exclusively via a 1,4-elimination process (Scheme III), and Co^+ should dehydrogenate *n*-pentane >90% (the value observed for butane) by Scheme III to produce the bis(olefin) complex VII. While Fe^+ is expected to dehydrogenate *n*-pentane

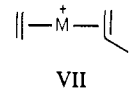

VII

>30% (the value observed for butane) by Scheme III, a substantial amount of dehydrogenation by Scheme II is also expected, producing a mixture of bis(olefin) and monoolefin products.

The CID spectra of $MC_5H_{10}^+$ ions generated in reaction 15 are similar to those for $MC_5H_{10}^+$ ions formed in reaction 14 with the exception that no loss of CH_4 is observed. While observation of CH_4 loss is, therefore, characteristic of the monoolefin structure VI, reproducibility of such a low abundance product (<5%) makes quantitation of the monoolefin vs. the bis(olefin) structure virtually impossible. Similarly, due to the low limit of detection (~3% of main peak) of the experiment, the absence of CH_4 from CID of $MC_5H_{10}^+$ ions from reaction 15 does not rule out the presence of some monoolefin complex. In summary, CID of $MC_5H_{10}^+$ complexes yields little structural information since the primary pentene structure VI rearranges readily to the bis(olefin) structure VII prior to dissociation.

Specific ion–molecule reactions can be used for ion structure determination. HCN displaces C_2H_4 and C_3H_6 sequentially from $CoC_5H_{10}^+$ ions generated in reaction 15 to produce $Co(HCN)_2^+$ ions (reaction 16). Displacement of C_3H_6 was considerably slower

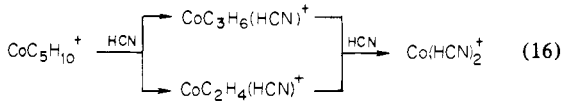

$$CoC_5H_{10}^+ \xrightarrow{HCN} \begin{cases} CoC_3H_6(HCN)^+ \\ CoC_2H_4(HCN)^+ \end{cases} \xrightarrow{HCN} Co(HCN)_2^+ \qquad (16)$$

than that for C_2H_4. HCN displaced C_2H_4 from both $FeC_5H_{10}^+$ and $NiC_5H_{10}^+$ ions generated in reaction 15 to produce $MC_3H_6(HCN)^+$ ions with only a trace of C_3H_6 displacement. Benzene was observed to displace either C_2H_4 or C_3H_6 equally from $CoC_5H_{10}^+$ and $NiC_5H_{10}^+$ ions formed in reaction 15 to produce $M(C_3H_6)(C_6H_6)^+$ and $M(C_2H_4)(C_6H_6)^+$ complexes (reaction 17). A second benzene displacement was also observed;

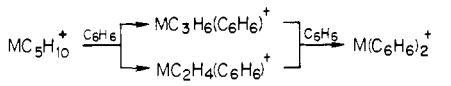

$$MC_5H_{10}^+ \xrightarrow{C_6H_6} \begin{cases} MC_3H_6(C_6H_6)^+ \\ MC_2H_4(C_6H_6)^+ \end{cases} \xrightarrow{C_6H_6} M(C_6H_6)_2^+ \qquad (17)$$

however, it was considerably slower than the initial displacement, possibly due to the quasi-coordinative saturation of the initial benzene–olefin complex. Only a trace (~1%) of displacement of C_5H_{10} from Co^+ or Ni^+ by benzene to form $MC_6H_6^+$ was observed. Reaction of benzene with $FeC_5H_{10}^+$ formed in reaction 15 is similar to $CoC_5H_{10}^+$ and $NiC_5H_{10}^+$; however, greater initial displacement of C_5H_{10} (~20%) to form $FeC_6H_6^+$ was observed, which is consistent with the presence of some linear pentene as expected.

Surprisingly, reaction of $CoC_5H_{10}^+$, generated in reaction 14, with HCN resulted in sequential displacement of C_2H_4 and C_3H_6 producing a $Co(HCN)_2^+$ ion analogous to reaction 16. In addition, HCN displaced only C_2H_4 from both $FeC_5H_{10}^+$ and $NiC_5H_{10}^+$ ions generated in reaction 14 to produce $MC_3H_6(HCN)^+$ ions. Although this suggests prior rearrangement of the monoolefin complex VI to the bis(olefin) complex VII, an alternative explanation is that HCN adds to $MC_5H_{10}^+$ forming an activated complex (reaction 18). This activated complex can then rearrange

$$MC_5H_{10}^+ + HCN \rightarrow (MC_5H_{10}(HCN)^+)^* \qquad (18)$$

to the bis(olefin) structure via Scheme VII, which can then eliminate either C_2H_4 or C_3H_6 for Co^+ or C_2H_4 for Fe^+ and Ni^+. If in fact rearrangement occurs after ligand attachment, then the use of a multicoordinating ligand may make this metal-centered rearrangement less facile due to the reduced availability of the coordination sites for rearrangement to take place. Benzene was used to test this idea. When this reaction is carried out, direct displacement of C_5H_{10} dominated (>50%) over loss of either C_2H_4 or C_3H_6 for all the $MC_5H_{10}^+$ ions generated in reaction 14. Benzene reacted similarly with $MC_5H_{10}^+$ ions generated by displacement of smaller olefins by 1-pentene. These results are in contrast to the benzene displacement reactions for $MC_5H_{10}^+$ ions produced in reaction 15 where little displacement of C_5H_{10} is observed; about 1% for Co^+ and Ni^+ and about 20% for Fe^+. This indicates that the majority of $MC_5H_{10}^+$ ions generated in reaction 14 have not rearranged to the bis(olefin) complex, VII. Furthermore, the benzene displacement reactions indicate that $MC_5H_{10}^+$ ions generated in reaction 15 for Ni^+ and Co^+ consist predominantly of the bis(olefin) structure while a considerable amount of the linear pentene structure is also present for this reaction with Fe^+.

$MC_6H_{12}^+$ Ions. $MC_6H_{12}^+$ ions are produced in the cleavage of linear alkanes larger than heptane by Fe^+, Co^+, and Ni^+ (reaction 19) to produce a 1-hexene–metal ion complex. The

$$M^+ + n\text{-}C_nH_{2n+2} \rightarrow MC_6H_{12}^+ + C_{n-6}H_{2n-10} \qquad (19)$$

fragment ion abundances vs. ion kinetic energy for CID of both $FeC_6H_{12}^+$ and $CoC_6H_{12}^+$ ions generated by reaction with *n*-octane are shown in Figure 6. Loss of C_3H_6 dominates for all $MC_6H_{12}^+$ ions and occurs via initial insertion into an allylic C–C bond (Scheme VII), producing a bis(propene)–metal ion complex that then loses C_3H_6. Loss of C_2H_4 and C_2H_6 (or $C_2H_4 + H_2$) are also observed. The $NiC_6H_{12}^+$ ions generated in reaction 19 only lose C_3H_6 under CID conditions. Again, no dehydrogenation to produce $MC_6H_{10}^+$ ions is observed. Loss of C_2H_4 produces a metal ion–butene complex. This ion may then dehydrogenate to form a metal ion–butadiene complex provided it retains sufficient internal energy. Loss of C_2H_6 (ethane) also will produce a metal ion–butadiene complex. Both of these processes probably contribute to formation of $MC_4H_6^+$ ions (Scheme VIII). Again, insertion into the allylic C–C bond is preferred over insertion into C–C bonds further removed from the double bond, even though the latter would produce thermally more stable products.[43]

The above CID results can be compared with the primary reaction products resulting from reaction of Fe^+, Co^+, and Ni^+

Scheme VIII

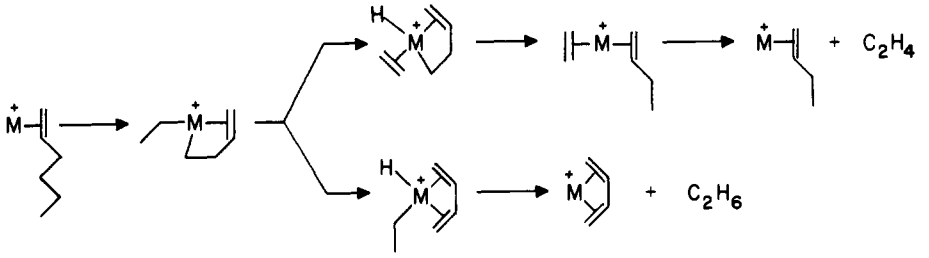

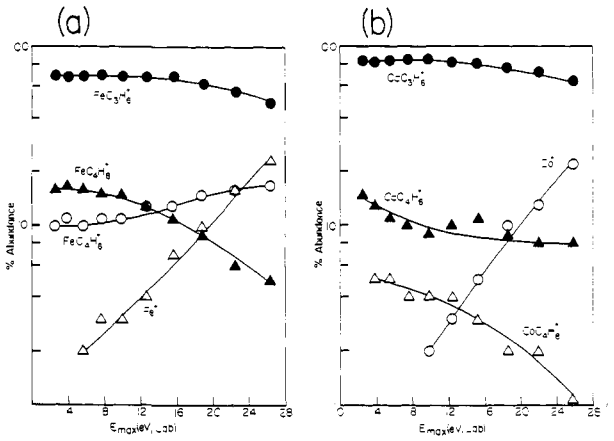

Figure 6. (a) CID product ion intensities vs. kinetic energy for $FeC_6H_{12}^+$ ions generated from *n*-octane (reaction 19). (b) CID product ion intensities vs. kinetic energy for $CoC_6H_{12}^+$ ions generated from *n*-octane (reaction 19).

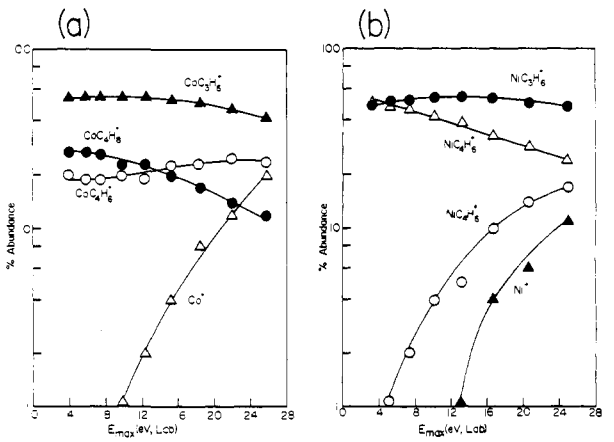

Figure 7. (a) CID product ion intensities vs. kinetic energy for $CoC_6H_{12}^+$ ions generated from *n*-hexane (reaction 20). (b) CID product ion intensities vs. kinetic energy for $NiC_6H_{12}^+$ ions generated from *n*-hexane (reaction 20).

with 1-hexene (Table II). These results are similar to the CID spectra in Figure 6; however, dehydrogenation and loss of CH_4 and C_4H_8 are also observed in these reactions. Again, these losses may be due to the metal ion inserting into C–H or C–C bonds prior to coordination to the C–C double bond. Loss of CH_4 produces a 1,4-pentadiene–metal ion complex in an exothermic reaction, which may rearrange to a conjugated diene. The formation of $MC_4H_6^+$, a metal ion–butadiene complex, generated in an exothermic reaction deserves further comment. This ion may be generated via loss of C_2H_6 (ethane) or loss of C_2H_4 followed by dehydrogenation. Loss of ethane requires that $D(^+M–C_4H_6) > 16$ kcal/mol to be exothermic while loss of $C_2H_4 + H_2$ requires $D(^+M–C_4H_6) > 49$ kcal/mol.[43] Bond energies of 1,3-alkadienes are about 45–60 kcal/mol for Co^+[4] with Fe^+ and Ni^+ probably being in this range, also. Hence, $MC_4H_6^+$ ions are believed to be formed via loss of ethane since loss of $C_2H_4 + H_2$ would be nearly thermoneutral while loss of C_2H_6 would be exothermic. Formation of $CoC_4H_6^+$ ions by reaction of Co^+ with 1-hexane in an ion beam instrument[8a] was reported to be formed via an endothermic reaction, contrary to our findings.

$MC_6H_{12}^+$ ions are formed in the dehydrogenation of hexane by Fe^+, Co^+, and Ni^+ (reaction 20). By analogy to the dehy-

$$M^+ + n\text{-hexane} \rightarrow MC_6H_{12}^+ + H_2 \qquad (20)$$

drogenation of both *n*-butane and *n*-pentane discussed above, Co^+ and Ni^+ will dehydrogenate *n*-hexane nearly exclusively via Scheme III, producing bis(olefin) products while Fe^+ should dehydrogenate *n*-hexane by both Schemes II and III, generating monoolefin and bis(olefin) products. No structural information was available for $FeC_6H_{12}^+$ ions generated in reaction 20 since the monoolefin and bis(olefin) structures cannot readily be distinguished by CID or ion–molecule reactions. The CID fragment ion abundances vs. kinetic energy for both $CoC_6H_{12}^+$ and $NiC_6H_{12}^+$ ions generated in reaction 20 are shown in Figure 7. The CID results provide evidence for two different bis(olefin) structures, VIII and IX. Structure VIII simply loses C_3H_6 while

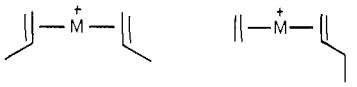

VIII IX

structure IX loses both C_2H_4 and $C_2H_4 + H_2$ in its CID spectra. The data suggest 48 ± 10% structure VIII and 52 ± 10% structure IX for both Co^+ and Ni^+. It is interesting that loss of $C_2H_4 + H_2$ is competitive with loss of C_2H_4 at all energies for Co^+. This is in contrast to Ni^+, where C_2H_4 loss dominates over the multiple loss product, $C_2H_4 + H_2$, even at high kinetic energies. This indicates that β-hydride transfers are considerably more facile for Co^+ complexes than for Ni^+ complexes. This is probably due to a low activation barrier for β-hydride transfers for Co^+, which is consistent with observation of reversible β-hydride shifts for reactions of Co^+ with deuterated alkanes.[4] This low activation barrier for β-hydride shifts may also explain why little $CoC_4H_8^+$ is produced in reaction 8, with $CoC_4H_6^+$ dominating instead in reaction 9. Formation of the metal ion–butadiene complex from IX may also proceed via loss of C_2H_6 (ethane). In this case, a β-hydrogen migrates across the metal from butene to generate an alkyl π-allyl–metal ion complex. This is followed by a second β-hydride shift across the metal, resulting in reductive elimination of ethane producing a metal ion–butadiene complex. Both processes may contribute to the formation of $MC_4H_6^+$ ions from IX.

$MC_7H_{14}^+$. Dehydrogenation of heptane by Fe^+, Co^+, and Ni^+ produces an $MC_7H_{14}^+$ ion (reaction 21). Again, Co^+ and Ni^+

$$M^+ + n\text{-heptane} \rightarrow MC_7H_{14}^+ + H_2 \qquad (21)$$

will dehydrogenate *n*-heptane essentially via Scheme III producing bis(olefin) products, and Fe^+ should dehydrogenate *n*-heptane via both Schemes II and III producing monoolefin and bis(olefin) products. CID failed to distinguish $FeC_7H_{14}^+$ isomers due to facile rearrangement of the monoolefin structures to bis(olefin) structures. The fragment ion abundances vs. ion kinetic energy for CID of $CoC_7H_{14}^+$ ions are shown in Figure 8. The CID results indicate the presence of two unique bis(olefin) complexes, X and XI, generated by Scheme III for both Co^+ and Ni^+. The data suggest 62 ± 10% structure X and 38 ± 10% structure XI for Co^+ and 85 ± 10% structure X and 15 ± 10% structure XI for

Table III. Neutral Products Lost in the Primary Reactions of Fe^+, Co^+, and Ni^+ with Linear Alkanes[a]

		neutral fragments lost, %									
alkane	M^+	H_2	CH_4	C_2H_6	C_3H_8	C_4H_{10}	C_5H_{12}	$2H_2$	CH_4, H_2	C_2H_6, H_2	C_3H_8, H_2
propane	Fe	24	76								
	Co	69	31								
	Ni	20	80								
butane	Fe	8	29	60				3			
	Co	18	8	74							
	Ni	12	4	84							
pentane	Fe	16	22	15	43				4		
	Co	19	2	67	10				2		
	Ni	37	2	44	17						
hexane	Fe	27	13	11	11	31				7	
	Co	23	1	24	31	7				14	
	Ni	36		22	27	8				7	
heptane	Fe	27	11	6	13	16	20				7
	Co	15		9	25	37	4				10
	Ni	24		12	32	22	5				5

[a] Alkane pressure 3×10^{-7} torr. Argon added for a total pressure of 1×10^{-5} torr. All numbers are ±10% of absolute. Values for Ni^+ are obtained from ref 11.

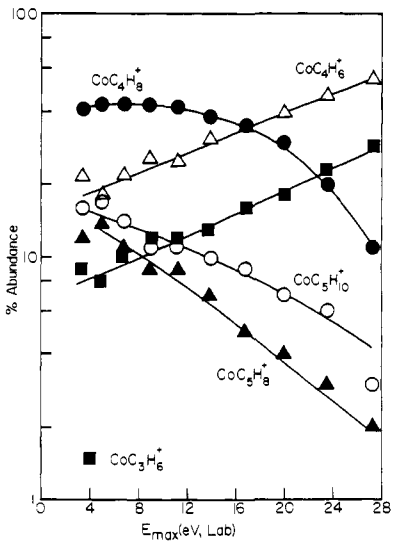

Figure 8. CID product ion intensities vs. kinetic energy for $CoC_7H_{14}^+$ ions generated from *n*-heptane (reaction 21).

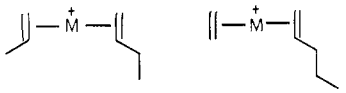

X XI

Ni^+. Structure X loses C_3H_6 and $C_3H_6 + H_2$ or C_3H_8 at low energy to produce $MC_4H_8^+$ and $MC_4H_6^+$, respectively. At higher energies, loss of C_4H_8 may occur, producing $MC_3H_6^+$; however, this is expected to be a minor contribution to the total $MC_3H_6^+$ ion intensity since larger alkenes are bound more strongly to metal ion centers than smaller alkenes.[42] Hence, the smaller alkene will be preferentially cleaved. Again, formation of $CoC_4H_6^+$ is competitive with $CoC_4H_8^+$ formation, even at low energies. This is consistent with facile β-hydride transfers for Co^+ complexes.

$MC_5H_{10}^+$ ions are generated by cleavage of C_2H_4 from structure XI. Surprisingly, a $CoC_5H_8^+$ ion is also observed. This could be generated by either cleavage of C_2H_4 followed by dehydrogenation or direct loss of C_2H_6 (ethane) by two successive β-hydride shifts. The $MC_5H_{10}^+$ ions produced by loss of C_2H_4 can rearrange to the bis(olefin) complex via Scheme VII with loss of C_2H_4 to produce $MC_3H_6^+$ ions. The increase in the intensity of $CoC_3H_6^+$ is roughly equal to the decrease in both $CoC_5H_{10}^+$ and $CoC_5H_8^+$ ion intensities, indicating that they are coupled.

Comparison of Reactivity. Product distributions for the primary reactions of Fe^+, Co^+, and Ni^+ with several linear alkanes, C_3–C_7, are presented in Table III. These results are in good agreement with those obtained previously for Fe^+ by using a conventional ICR spectrometer[2b] and for Fe^+, Co^+, and Ni^+ at ~1 eV of kinetic energy reported by using an ion beam instrument.[7] All three metal ions dehydrogenate propane exclusively by a 1,2-elimination process (Scheme II). Ni^+ dehydrogenates linear alkanes larger than propane exclusively via a 1,4-elimination process (Scheme III), and this mechanism also dominates for Co^+. A true dichotomy exists for the dehydrogenation of linear alkanes larger than propane by Fe^+, however, with both Schemes II and III being involved. Insertion into C–C bonds is considerably more facile than insertion into C–H bonds for all three metal ions.

Table IV. Bond Dissociation Energies (kcal/mol) for M^+–R Species

bond energies	Fe^+	Co^+	Ni^+
$D^0(M^+-H)$	58 ± 5[a]	52 ± 4[b]	43 ± 2[c]
$D^0(M^+-CH_3)$	69 ± 5[d]	61 ± 4[b]	48 ± 5[d]
$D^0(M^+-H) + D^0(M^+-CH_3)$	127	113	91
$2D^0(M^+-CH_3)$	138	122	96

[a] Reference 5. [b] Reference 4. [c] Reference 7. [d] Reference 3.

Table V. Bond Dissociation Energies (kcal/mol) for Organic Species[a]

bond	energy	bond	energy
H-*n*-C_3H_7	98	CH_3–CH_3	88
H-*i*-C_3H_7	95	CH_3CH_2–CH_3	85
H-*sec*-C_4H_9	95	$CH_3CH_2CH_2$–CH_3	85
H-allyl	89	CH_3CH_2–CH_2CH_3	82[b]

[a] Values taken from "CRC Handbook of Chemistry and Physics", 55th ed.; The Chemical Rubber Co.: Cleveland, Oh, 1974; pp F-213-215. [b] Calculated from ref 43.

The above results may be explained qualitatively by using the thermochemistry in Tables IV and V. The enthalpy change for metal insertion (eq 22) is related to the various bond dissociation

$$M^+ + R_1R_2 \rightarrow R_1\text{–}M^+\text{–}R_2 \quad (22)$$

$$\Delta H \simeq D(R_1\text{–}R_2) - D(R_1M^+\text{–}R_2) - D(M^+\text{–}R_1) \quad (23)$$

energies by eq 23. The Ni^+–H bond dissociation energy is 43 ± 2 kcal/mol, and the Ni^+–CH_3 bond dissociation energy is 48 ± 5 kcal/mol. Assuming that the latter is a typical Ni–alkyl bond strength and that the above energies are unaffected by the addition of a second ligand (H or alkyl) to the metal ion and using D(C–H) = 95 kcal/mol and D(C–C) = 85 kcal/mol, then insertion of Ni^+ into C–H bonds would be slightly endothermic by ~4 kcal/mol and insertion into C–C bonds would be exothermic by ~11 kcal/mol. By the same arguments, insertion of Co^+ into C–H and C–C bonds is exothermic by ~18 and ~37 kcal/mol, respectively, and insertion of Fe^+ into C–H and C–C bonds is also exothermic by ~32 and ~53 kcal/mol, respectively.

Reactions of Co^+ and Ni^+ with propane are considerably slower than those for larger alkanes which approach the Langevin rate. This slow reaction may allow insertion into C–H bonds to become

Table VI. Selective Insertion into C–C Bonds of Linear Alkanes by Fe^+, Co^+, and Ni^+ [a-c]

alkane	M^+	carbon bond insertion, % 1	2	3
	Fe	33	67	
	Co	8 (10)	92 (90)	
	Ni	4 (5)	96 (95)	
	Pre	67	33	
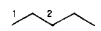	Fe	31	69	
	Co	4 (5)	96 (95)	
	Ni	2 (3)	98 (97)	
	Pre	50	50	
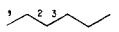	Fe	17	69	14
	Co	1 (1)	57 (59)	42 (40)
	Ni	0 (0)	54 (58)	46 (42)
	Pre	40	40	20
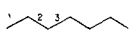	Fe	15	36	49
	Co	0 (0)	19 (15)	81 (84)
	Ni	0 (0)	21 (22)	79 (78)
	Pre	33	33	33

[a] Pre = predicted percentages based on nonselective insertion. [b] Dehydrogenation products for Fe^+ are not included. [c] Values in parentheses do not include dehydrogenation products.

Table VII. Fraction of Dehydrogenation vs. Alkane Loss (H_2/Alkane Loss) for Each Internal Carbon Bond Cleaved

alkane	M^+	carbon bond cleaved 2	3
	Fe	0.04	
	Co	0.22	
	Ni	0.14	
	Co	0.24	
	Ni	0.61	
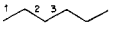	Co	0.22	0.24
	Ni	0.55	0.57
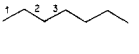	Co	0.27	0.11
	Ni	0.17	0.35

Scheme IX

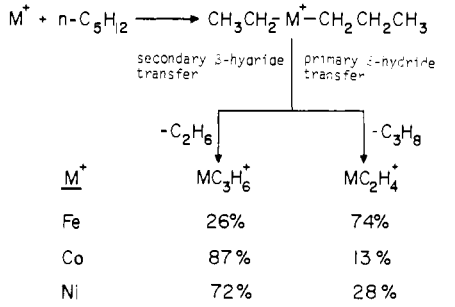

competitive with insertion into C–C bonds of propane but not of larger alkanes. Insertion into C–H bonds is completely absent for Ni^+, and only a trace is seen for Co^+ in reactions with *n*-butane. This observation is not surprising for Ni^+; however, insertion of Co^+ into C–H bonds is expected to be roughly as exothermic as that for Ni^+ insertion into C–C bonds. Fe^+ reacts rapidly with both propane and butane, with facile insertion into both C–H and C–C bonds being observed. The facile insertion of Fe^+ into C–H bonds is expected on the basis of the energetics described above.

Formation of $MC_4H_6^+$ ions occurs for all three metal ions upon reaction with larger alkanes (Table III). These ions must be formed via multiple neutral fragment losses. In most cases, a variety of different neutral fragment losses may be postulated for $MC_4H_6^+$ formation. It is also important to know the order in which these losses occur. As a specific example, the $MC_4H_6^+$ ions generated by reaction with *n*-hexane may be formed via the following multiple losses: $2CH_4$ or C_2H_6 and H_2. From the CID results, it is clear that $MC_4H_8^+$ ions generated by cleavage of C_2H_6 from *n*-hexane readily dehydrogenate to produce $MC_4H_6^+$ ions. Loss of CH_4 to produce $MC_5H_{10}^+$, however, is observed only as a minor product in the reaction of M^+ with *n*-hexane. Furthermore, loss of CH_4 from $MC_5H_{10}^+$ to produce $MC_4H_6^+$ is also a minor CID product. It seems clear that in this case $MC_4H_6^+$ ions result from loss of C_2H_6 followed by dehydrogenation and not from two successive CH_4 losses. In general, $MC_4H_6^+$ ions generated by reactions with linear alkanes larger than *n*-butane are formed by initial loss of an alkane producing $MC_4H_8^+$, a linear butene–metal ion complex, which then dehydrogenates forming $MC_4H_6^+$.

The product distributions listed in Table III can be used to determine the relative frequency of insertion into particular C–C bonds by the metal ions (Table VI). Multiple alkane/H_2 loss products are included, and the dehydrogenation products for both Co^+ and Ni^+ are included in the data for Table VI since these involve initial C–C bond cleavage while dehydrogenation products generated by Fe^+ are ignored since both C–C and C–H bond insertions are involved. For comparison with the Fe^+ data, the values obtained when the dehydrogenation products for Ni^+ and Co^+ are ignored are also included in Table VI. The small deviations observed for Ni^+ and Co^+ under these conditions suggest that omitting the dehydrogenation products for Fe^+ will not significantly affect the data in Table VI.

The results in Table VI can be compared with a completely random or nonselective mode of metal insertion into C–C bonds. Co^+ and Ni^+ are both highly selective against insertion into terminal C–C bonds, with Fe^+ being considerably less selective. There are two main factors involved in this selectivity. First, terminal C–C bonds are approximately 3 kcal/mol stronger than internal C–C bonds; hence, terminal bonds are more difficult to cleave. Secondly, metal–alkyl bonds should become stronger as the size of the alkyl chain increases, due to electronic considerations. Both of these factors contribute to discriminate against terminal C–C bond insertion.

The increasing selectivity from Fe^+ to Ni^+ is consistent with decreasing $M–CH_3^+$ bond strengths (Table III). Surprisingly, the selectivity of Co^+ parallels that of Ni^+, even though the $Co^+–CH_3$ bond strength is 13 kcal/mol stronger than that for $Ni^+–CH_3$. One possible explanation for this observation is that a second alkyl group has a greater effect on the overall metal–alkyl bond strength for Co^+ than Ni^+. This seems to imply that the dissociation energy for cleavage for two alkyls from Co^+ is roughly equal to that for Ni^+ (eq 24).

$$D(^+CoR_1–R_2) + D(^+Co–R_1) \simeq D(^+NiR_1–R_2) + D(^+Ni–R_1) \quad (24)$$

Dehydrogenation of linear alkanes larger than propane by a 1,4-elimination process (Scheme III) requires that β-hydride shifts be competitive with alkane elimination. Table VII lists the ratio of dehydrogenation vs. alkane loss for each particular internal C–C bond cleaved for linear alkanes, C_4–C_7, by using data from Tables III and VI. The results indicate that dehydrogenation via Scheme III is least competitive with alkane elimination for Fe^+ reacting with *n*-butane. For Ni^+, dehydrogenation becomes more competitive with alkane elimination when secondary β-hydrogens are involved; however, Co^+ shows no such relationship.

The cleavage of alkanes by metal ions, Scheme I, involves β-hydride transfers. The competition between secondary and primary β-hydride transfer can be studied in specific cases. Insertion of a metal ion into the internal C–C bond of *n*-pentane produces an intermediate that contains both primary and secondary β-hydrogens. Transfer of a secondary β-hydrogen results in elimination of ethane while transfer of a primary β-hydrogen results in loss of propane (Scheme IX). For both Co^+ and Ni^+, transfer of a secondary β-hydrogen is preferred. This is reversed for Fe^+, however, where transfer of a primary β-hydrogen is dominant. The results for Fe^+ are surprising since a primary C–H bond is roughly 3 kcal/mol stronger than a secondary C–H bond. Hence, the facile transfer of primary β-hydrogens by Fe^+ is probably related to kinetic rather than thermodynamic considerations. Facile primary β-hydrogen transfers also hold for insertion of Fe^+ into the secondary C–C bond of *n*-hexane, where loss of C_4H_{10} (primary β-hydrogen transfer) is dominant over loss of C_2H_6 (secondary β-hydrogen transfer).

Conclusions

The group 8 transition-metal ions Fe^+, Co^+, and Ni^+ all show similar reactivity with linear alkanes. Differences in reactivity can be understood by considering the thermochemistry in Tables IV and V. All three metal ions dehydrogenate linear alkanes via initial insertion into C–C bonds (Scheme III), producing a bis(olefin) complex. In addition, Fe^+ also dehydrogenates linear alkanes via initial insertion into C–H bonds (Scheme II).

Collision-induced dissociation (CID) is a powerful technique for studying the structures of organometallic complexes and hence yielding mechanistic information on ion product formation. In addition, a variety of fundamental chemical information is available from studying the CID fragmentation pathways of known structures. Ligand rearrangements are encountered in CID of olefins larger than butene bound to metal ion centers. Therefore, caution must be exercised in interpreting the CID spectra of organometallic ions since the observation of cleavage products does not necessarily imply attachment of that species directly onto the metal. This also holds for interpretation of ion–molecule reactions where the ion–molecule reaction complex may contain sufficient internal energy for rearrangement to occur prior to displacement. In the case of organometallic species, displacement by multicoordinating ligands such as benzene may occupy sufficient coordination sites that can, in turn, decrease metal-centered rearrangements.

We are currently studying the reactions of Fe^+, Co^+, and Ni^+ with a host of branched alkanes, olefins, and ketones. Determination of product structures will aid in the elucidation of reaction mechanisms. Secondary and tertiary reactions are also being investigated for olefins and ketones. In addition, we are also looking at the chemistry of the second- and third-row group 8 transition-metal ions.

Acknowledgment is made to the Department of Energy (DE-AC02-80ER10689) for supporting this research and the National Science Foundation (CHE-8002685) for providing funds to purchase the FT MS.

Registry No. Fe^+, 14067-02-8; Co^+, 16610-75-6; Ni^+, 14903-34-5; 1-pentene, 592-41-6; 1-hexene, 592-41-6; propane, 74-98-6; butane, 106-97-8; pentane, 109-66-0; hexane, 110-54-3; heptane, 142-82-5; 2,2-dimethylpropane, 463-82-1.

Picosecond Laser Photolysis Studies of Deactivation Processes of Excited Hydrogen Bonding Complexes. 3. Detection of the Nonfluorescent Charge-Transfer State in the Excited 1-Aminopyrene–Pyridine Hydrogen Bonded Pair and Related Systems†

Noriaki Ikeda, Hiroshi Miyasaka, Tadashi Okada, and Noboru Mataga*

Contribution from the Department of Chemistry, Faculty of Engineering Science, Osaka University, Toyonaka, Osaka 560, Japan. *Received December 20, 1982*

Abstract: The mechanism of the fluorescence quenching observed when two conjugated π-electron systems are directly combined by hydrogen bonding has been studied in the case of the 1-aminopyrene–pyridine system by means of the picosecond laser photolysis method. Time-resolved transient absorption spectra were observed for the excited hydrogen bonded pair and fluorescence decay curves of 1-aminopyrene in the presence of pyridine were determined by means of a picosecond streak camera. It has been confirmed that a rapid equilibrium between the locally excited state (D^*–H···A) and the charge-transfer state (D^+–H···A^-) of the hydrogen bonded pair is realized within the time resolution of our picosecond apparatus. It has been established that the fluorescence quenching in the 1-aminopyrene–pyridine system is due to the formation of a nonfluorescent charge-transfer state in the excited hydrogen bonded pair. In relation to these studies, it has been demonstrated that, although the fluorescence of *N,N*-dimethyl-1-aminopyrene in nonpolar solvents is not affected by added pyridine, indicating the crucial importance of the hydrogen bonding for the charge transfer to occur, it forms a short-lived nonfluorescent exciplex with 4-cyanopyridine which is a much weaker proton acceptor but a stronger electron acceptor than pyridine.

Inter- and intramolecular hydrogen bonding interactions can affect rather drastically the photophysical and photochemical properties of a large number of molecular systems. It is well-known that hydrogen bonding interaction frequently leads to the quenching of fluorescence, especially when two conjugate π-electronic systems are directly combined by hydrogen bonding interaction.[1-4]

CT (charge transfer) interaction between proton-donor and -acceptor π-electron systems via the hydrogen bond was suggested as a possible mechanism of the quenching.[1] Namely, a kind of nonfluorescent exciplex was assumed to be formed in the course of this quenching process. Hydrogen atom transfer from proton donor to acceptor in the hydrogen bonded pair was also suggested as a possible mechanism of quenching.[2]

In relation to this problem, we have undertaken a systematic picosecond (ps) laser photolysis study of a series of conjugated π-electronic hydrogen bonding systems, in view of the importance of this problem in elucidating the photochemical and photobiological primary processes. We have detected for the first time the formation of a transient CT state in the excited state of several conjugated π-electronic hydrogen bonding systems.[5-8] In this paper results of 1-aminopyrene–pyridine and related systems will be reported.

† Parts 1 and 2 of this series are published respectively in ref 5b and 6.

(1) (a) Mataga, N.; Tsuno, S. *Naturwissenschaften* **1956**, *10*, 305. (b) Mataga, N.; Tsuno, S. *Bull. Chem. Soc. Jpn.* **1957**, *30*, 711. (c) Mataga, N. *Ibid.* **1958**, *31*, 481. (d) Mataga, N.; Torihashi, Y.; Kaifu, Y. *Z. Phys. Chem. (Frankfurt/Main)* **1962**, *34*, 379. (e) Mataga, N.; Tanaka, F.; Kato, M. *Acta Phys. Pol.* **1968**, *34*, 733.

(2) Rehm, D.; Weller, A. *Isr. J. Chem.* **1970**, *8*, 259.

(3) (a) Kikuchi, K.; Watarai, H.; Koizumi, M. *Bull. Chem. Soc. Jpn.* **1973**, *46*, 749. (b) Yamamoto, S.; Kikuchi, K.; Kokubun, H. *Ibid.* **1976**, *49*, 2950.

(4) Martin, M. M.; Ware, W. R. *J. Phys. Chem.* **1978**, *82*, 2770.

(5) (a) Ikeda, N.; Okada, T.; Mataga, N. *Chem. Phys. Lett.* **1980**, *69*, 251. (b) Ikeda, N.; Okada, T.; Mataga, N. *Bull. Chem. Soc. Jpn.* **1981**, *54*, 1025.

(6) Martin, M. M.; Ikeda, N.; Okada, T.; Mataga, N. *J. Phys. Chem.* **1982**, *86*, 4148.

(7) Ikeda, N.; Okada, T.; Mataga, N., to be published elsewhere.

(8) Ikeda, N.; Nishida, T.; Mataga, N. to be published elsewhere.

0002-7863/83/1505-5206$01.50/0